Vibrational Spectroscopy 119 (2022) 103341

Contents lists available at ScienceDirect

Vibrational Spectroscopy

journal homepage: www.elsevier.com/locate/vibspec

Pb intoxicated biomolecular changes in *Cladonia convoluta* studied using 2DCOS infrared spectroscopy coupled with chemometric analysis

Sivakumaran Karthikeyan [a], Rafig Gurbanov [b,*], Dilek Unal [c]

[a] Department of Physics, Dr. Ambedkar Government Arts College, Chennai, 600039, Tamil Nadu, India
[b] Department of Bioengineering, Bilecik Şeyh Edebali University, 11230, Bilecik, Turkey
[c] Department of Molecular Biology and Genetics, Bilecik Şeyh Edebali University, 11230, Bilecik, Turkey

ARTICLE INFO

Keywords:
2DCOS
Lichens
Polysaccharides
ROC
Pb

ABSTRACT

Lead (Pb) is used in many industrial applications and is a toxic heavy metal that causes health hazards. Lichens are symbiotic associations that are environment friendly in removing toxic elements from the polluted environment. They can accumulate heavy metals and are therefore considered in biomonitoring of metal pollution. In this study, biochemical markers due to lead toxicity on *Cladonia convoluta* were revealed using two-dimensional correlation (2DCOS) spectra analysis. The 2DCOS enhances the resolution of the spectrum and gives more information on the interaction of functional groups within and between molecules which cannot be revealed from conventional spectra. Thus, 2DCOS is an efficient tool in monitoring even minute spectral changes in complex spectra. The results of conventional IR analysis showed changes in the band area. It follows in the order polysaccharides > proteins > lipids due to lead toxicity. The results of 2D correlation spectra show predominant changes at the pyranose ring. The hetero asynchronous map show correlation changes of pyranose ring with lipid and proteins. It reveals a change in carbohydrate synthesis due to toxicity. The highest positive and negative PCA loading values show deformation pyranose ring to glucan band. The results of HCA show samples are well separated into two major clusters with high separation values. ROC analysis gives good reliability of the test. Hence, 2DCOS coupled with chemometric analysis helps in understanding the biomolecular changes *in C. convoluta* effectively.

1. Introduction

The increase of heavy metal pollution due to the growth of industrial activities results in environmental pollution. Lead (Pb) contamination arises from human activities (mining) and various factories. The toxic effect of Pb causes major concern to living beings. Hence, an efficient and cost-effective method is necessary to remove heavy metals from the environment. Fungi is environment friendly and cost-efficient in removing toxic elements from the polluted environment [1]. Lichens are symbiotic organisms consisting of at least one green microalgae or cyanobacteria and fungi, which are considered an indicator of environmental quality. They can accumulate a variety of contaminants such as heavy metals and radionuclides [2]. Bio sorbent can be effectively used in the removal of heavy metal ions from the wastewaters. The main advantage of this approach is its effectiveness in the reduction of pollutant concentration using low-cost biomass materials [3,4]. The biological effects of lichen polysaccharides are antitumor, immunomodulating, antiviral, etc. [5]. The immune-stimulating properties of polysaccharides, especially the β -glucans, enhance their capacity to the innate immune system and stimulate tumor rejection [6]. Hence, they are generally considered to be biological response modifiers. Besides the cell wall, extracellular polysaccharides attached to the cell surface are released into the surrounding, playing an important role in the sequestration of heavy metals [7,8]. The presence of charged groups in exopolysaccharides has been related to the capacity to sequestrate positively charged metals [9].

The fungal cell wall plays an important role in the physiological adaptation to its environment [10]. Carbohydrates are important for fungal metabolism by providing energy for synthesis. The other mechanism includes hyphal growth and amino acid biosynthesis [11]. The carbohydrate component of the cell wall has been demonstrated to have extensive applications in medicine [12]. It is an important biological molecule because of its role in energy storage in the form of glucose and starch. They support defense operations on the surface of cells and serve

* Corresponding author.
E-mail addresses: rafiq.qurbanov@gmail.com, rafig.gurbanov@bilecik.edu.tr (R. Gurbanov).

https://doi.org/10.1016/j.vibspec.2022.103341
Received 2 June 2021; Received in revised form 4 January 2022; Accepted 11 January 2022
Available online 13 January 2022

as the backbone of DNA. The common sugars have five and six-membered rings. Five-membered rings are called "furanoses" and six-membered rings are called "pyranoses". Certain sugars, of monosaccharide glucose, are called pyranoses having a six-membered tetrahydropyran rings structure. Glucan is a polysaccharide made up of repeating units of glucose monomers that are linked by glycosidic bonds. Alpha (α) linked glucans such as starch have their glucose units linked together by alpha glycosidic bonds. Beta (β) linked glucans, on the other hand, are linked by beta glycosidic bonds. The algae are composed of β-glucan and chitin. It provides mechanical strength and gives the cell its shape. The outer layer has proteins that are linked to the glucan and chitin network via glucan linkage. The cell wall contents have five main components: glucan, mannans, chitin, lipids, and proteins. Beta (β)-glucans and mannans are major components of the cell wall [13].

FTIR is a powerful tool in the study of biological samples due to the characteristics of functional groups exhibited by IR absorption. It is successfully employed for examining biological molecules [14]. Vibrational spectroscopy using MIR is a non-destructive analytical method that serves as spectral "biomarkers" to authenticate samples. IR spectra have unique molecular vibrational modes for each functional group. The composition and structure of functional groups can be determined from the position, width, and intensity of the spectra [15]. However, minute changes in peak positions and intensity changes cannot be observed from one-dimensional spectra. Hence, 2D correlation spectra are used which not only gives minute changes but also shows the correlation between frequencies. The synchronous and asynchronous correlation spectra show the variation of prominent band changes which cannot be observed from conventional 1D spectra. Thus, two-dimensional correlation spectroscopy (2DCOS) is an efficient tool in describing the structural changes in a molecular system. However, limited focus on lichens using 2DIR is established. Further, vibrational spectroscopy with chemometrics was successfully applied in the discrimination of chemical compositions of biological samples. In this study, principal component analysis (PCA) and hierarchical cluster analysis (HCA) were employed to explore the identification and classification of *Cladonia convoluta* species treated with various lead concentrations. Receiver operation characteristic (ROC) analysis was also done to demonstrate the accuracy of the experimental results. The use of spectral analysis with chemometrics allows getting maximum information from spectral data. Hence, the present study illustrates how the biomarker of lichens exhibits a defense mechanism due to Pb toxicity. The 2DCOS method coupled with chemometric techniques were used to demonstrate the biochemical compositional changes in *C. convoluta* thallus exposed to Pb intoxication.

2. Materials and methods

Cladonia convoluta lichen species were collected from the unpolluted area of Bilecik Central Forest, Turkey (N 40_ 11.′526′, E 029_ 57.′962′) and used for laboratory experiments. Samples were transferred to the laboratory in plastic bags and washed thrice with distilled water to remove dust from the surface. In this study, living lichen thallus was used to observe the biochemical changes due to lead stress and identify markers that may respond to lead stress. Each experimental group was designed as a collection of ten *C. convoluta* thallus. The thallus was incubated for 2 h in 250 mL of distilled water (as of Control), 0.5, 1.0, 1.5, 2.0, and 2.5 mM $Pb(NO_3)_2$ solution. After incubation, lichen thallus taken into Petri dishes were kept in the climate chamber for 72 h at 25 °C, under 16:8 light/dark cycle growth conditions, as described in our previous study [16]. The experiments were carried out with four replicates.

The physiological response in the lichen assay in response to lead treatment was determined by measuring lipid peroxidation and cell membrane integrity. Lipid peroxidation and membrane integrity analyses of thallus were performed according to Heath and Packer [17] and Garty et al. [18], respectively. The experiments were carried out with four replicates.

2.1. FTIR analysis

The infrared (IR) spectra of control and Pb-exposed lichen samples were obtained using FTIR Spectrometer (PerkinElmer, US) equipped with an ATR accessory. The lichen thallus was placed on a ZnSe crystal plate. The spectrum was recorded in the region 4000 to 500 cm^{-1}, with a resolution of 4 cm^{-1} with 32 scans.

2.2. Two-dimensional correlation method

Two-dimensional correlation spectra were constructed using 2D Shige v1.3 software [19–23]. It provides the correlation information between absorption peaks of one-to-one correspondence due to external perturbation. It gives the characteristics information of molecular changes with good sensitivity. Before executing 2D correlation, the FTIR data were smoothed, baseline corrected and normalized to 3300 cm^{-1}. The application of lead treatment was regarded as an external perturbation. The information obtained from the 2DCOS spectra gives characteristics information of the sample with good sensitivity.

2.3. Principal component analysis

The Principal Component Analysis (PCA) was done with SPSS 16.0 programming. It is used in multivariate data reduction. FTIR data are mean-centered, with second derivative and vector normalized before being subjected to PCA analysis. PCA was done in the region 4000–500 cm^{-1} for all samples. The output of the PCA results as scores and loadings [24]. It explains the maximum variation of the data present in the samples. The scores were plotted to show the variation from the FTIR spectra.

2.4. Receiver operation characteristics analysis

Receiver operation characteristics (ROC) is a statistical decision theory popularly growing in biological science. The study gives the effectiveness of different tests by a common unit called the area under the curve (AUC). To form the ROC curve, FTIR data obtained for treated samples were given as input variables and control taken as a reference point with a threshold of limit as 95 % using SPSS 16.0 software. The ROC plot was obtained for sensitivity against 1-specificity for each given input value. It helps to compare the overall experimental outcome of the test [25]. ROC results help determine the sensitivity and specificity associated with the chosen threshold limits (95 %) using SPSS 16.0 software. ROC curves allow us to select the best test carried out in the experiment.

2.5. Hierarchical cluster analysis

Hierarchical cluster analysis was performed by Ward algorithm using SPSS 16.0. Pearson's product-moment correlation coefficient with the squared Euclidean distance method using the Ward algorithm was applied using SPSS 16 Software. The results of the data are presented on a dendrogram scale. The clustering maximizes their similarity and minimizes the errors in distinguishing the samples [26]. The groups formed help in identifying the classification of results. The result is presented in a tree form.

2.6. Statistical analysis

Statistical evaluation of physiological data was done using One Way ANOVA (SPSS for Windows version 11.0). In addition, Pearson's correlation test was used to compare these data with the FTIR spectral band areas. The critical value for statistical significance is $p < 0.05$.

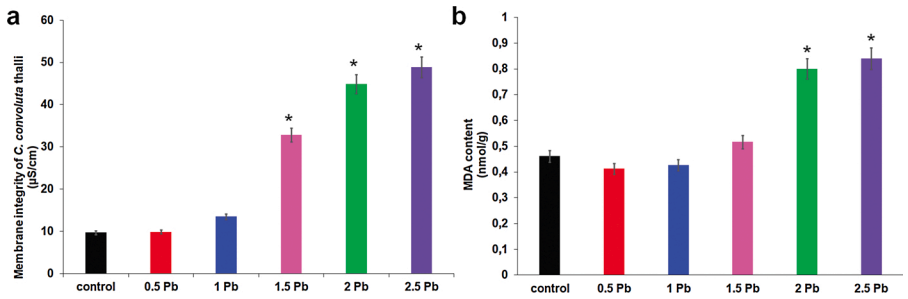

Fig. 1. (a) membrane integrity of *Cladonia convoluta* thalli. (b) lipid peroxidation rate of *C. convoluta* under different concentrations of Pb treatment and distilled water as a control, * represents $p < 0.05$.

3. Results and discussion

3.1. Physiological analysis of C. convoluta due to Pb toxicity

Lead causes different physiological responses in the photobiont layer compared to other elements, especially due to its entry into the photobiont at high concentrations after a long time of exposure [8,27]. Many studies have been carried out with various metals in lichens [8,15,24,25]. A previous study reports that the toxicity of short-term metal applications on photosynthetic capacity is Hg > Co > Cu, Cd > Pb, Ni [24]. Similarly, Sen et al. [25] demonstrated that short-term aluminum application negatively affects the lichen thallus within 24 h and significantly reduces the chlorophyll content. Although many metals have different effects on various types of lichen, they negatively affect the photosynthetic mechanism, in the first place. In addition, membrane stability measurement is frequently used for understanding the physiological conditions of lichen under metal stress [15]. The membrane integrity ratio is considered indicative of damage to cell membranes and has been previously used for the assessment of electrolyte leakage. Previous studies in higher plants have also shown that Pb binding to the cell wall or membrane components causes significant changes [28]. Therefore, the physiological responses to Pb were determined by membrane permeability and lipid peroxidation rate analyses in the present study (Fig. 1a and b). While the electrical conductivity (EC) value did not show a significant change in the samples treated with 0.5–1.0 mM Pb, it was determined that the membrane conductivity increased depending on the increase in the concentration of Pb (Fig. 1a). These changes in the conductivity of the cell wall can induce lipid peroxidation [28,29]. Similarly, it was determined that malondialdehyde (MDA), a biomarker of lipid peroxidation, was excessively produced in groups treated with 2.0–2.5 mM Pb (Fig. 1b). However, 0.5–1.5 mM Pb application did not significantly affect MDA content. In *Ramalina farinacea*, short-term (in hours) Pb administration has been shown to cause a decrease in lipid peroxidation [30]. In contrast, long-term (in days) exposures to Pb treatment in *Xanthoria parietina* or *Cladonia convoluta* thalli have been shown to have a positive correlation depending on the concentration of Pb [16,31]. In this respect, lipid peroxidation results are consistent with previous studies.

The methods used for physiological data are the most common ones, however, they do not show the detailed changes in macromolecular structure. In addition, many molecular methods used to understand the change in lipid, protein, and carbohydrates are studied by separating or culturing the fungus and algae components of the lichen structure [8]. Our knowledge on the determination of changes in the lichen thallus without separating the symbiotic association is very limited. From this point, we used the 2DCOS method to understand how Pb stress alters the membranes and macromolecules they contain without separating the lichen assembly.

3.2. Frequency assignment of FTIR spectra of C. convoluta due to Pb toxicity

Lichens have complex chemical compositions, and hence, IR spectra show a superposition of various absorption bands arising from different functional groups [32]. Fig. 2a. shows typical FTIR spectra of *Cladonia convoluta* species in the region 4000−500 cm^{-1}. Table 1 shows its characteristic frequency assignments. The spectra consist of several bands arising from the vibrations of different groups such as proteins, lipids, and carbohydrates. The most predominant changes in the bands are seen at spectral ranges 1800−900 cm^{-1}. This signifies that the *C. convoluta* are rich in biochemical compositions [16]. The weak intensities at ~ 3300 cm^{-1}, 2925 cm^{-1}, and 2851 cm^{-1} were assigned to Amide A of proteins, CH_2 asymmetric and symmetric stretching of lipids, respectively [33,34]. The band assigned to 1730 cm^{-1} corresponds to the C—O stretching of uronic acid (hydroxyl group of pyranose ring). The Amide I and Amide II bands correspond to 1630 cm^{-1} and 1539 cm^{-1} of proteins. Other bands were seen at 1370 cm^{-1} correlates with C—H bending and CO—H bending of a pyranose ring structure. The C—OH bending + CH_2 deformation corresponds to 1298 cm^{-1}. The intense peak at the 1032 cm^{-1} band corresponds to the C—C stretching of polysaccharides which is a major component of the *C. convoluta* [35].

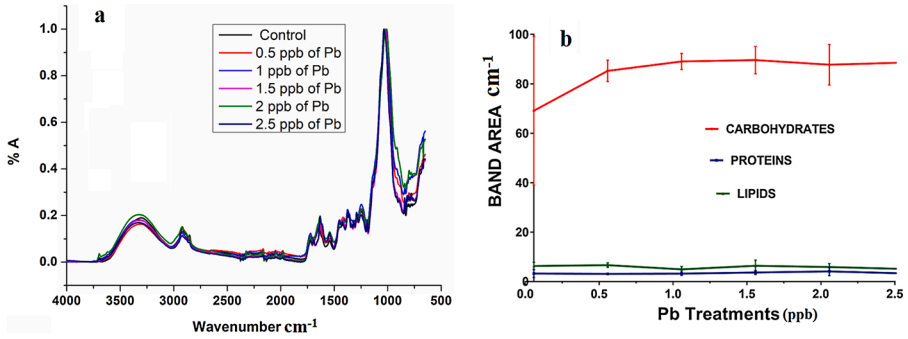

Fig. 2. (a) Representative FTIR spectra of *C. convoluta* in the region 4000-500 cm^{-1}. (b) Selected band area measurement of lipids (3000-2800 cm^{-1}), proteins (1705-1575 cm^{-1}), and carbohydrates (1200-900 cm^{-1}) for various Pb treatments of *C. convolute.*

Table 1
Tentative frequency assignment of *Cladonia convoluta*.

Wavenumber (cm^{-1})	Frequency assignment
3300(vw)	Amide A protein
2925(vw)	CH_2 asymmetric stretching lipids
2851(vw)	CH_2 symmetric stretching lipids
1730(vw)	C-O stretching uronic acid
1630(w)	Amide I protein
1539(w))	Amide II protein
1370(w)	C—H bending + C—OH bending Pyranose ring
1298(w)	C-OH bending + CH_2 deformation
1032(vs)	C-C stretching glycogen

vs-very strong, w- weak, vw-very weak.

3.3. Band area measurement of FTIR spectra of C. convoluta due to Pb toxicity

Fig. 2b shows the measured band areas for lipids (3000−2800 cm^{-1}), proteins (1705−1575 cm^{-1}), and carbohydrates (1200−900 cm^{-1}) at various Pb treatments [24,36]. The results show carbohydrates having the highest band area measured. Moreover, the intoxication of Pb resulted in an increased band area noted at 1 ppb of Pb treatment. No significant increase is noted after 1 ppb, and a plateau curve region was observed (Fig. 3). Carbohydrates are associated with fungal metabolism providing energy for synthesis and growth [11]. This signifies that carbohydrate metabolism is utilized as an immediate resource of energy under external stress. The lipids and proteins are the next parameters showing changes in the band area due to Pb treatment. Pearson's correlation results also showed that physiological response to lead stress was related to the protein and polysaccharide band areas (Table 2). The protein and polysaccharide band areas exhibited a strong positive correlation with membrane integrity rate. In contrast, the lipid peroxidation rate demonstrated weak and medium positive correlation with polysaccharide and protein band areas, respectively. Besides, the lipid band area showed a medium negative correlation with lipid peroxidation and membrane integrity. These results indicate that changes not only in cell wall polysaccharides but also in proteins could be important in tolerance to lead stress. Similarly, Lisette D'Souza et al. [37] studied the effect of Cd stress on *P. tetrastromatica* algae and showed evidence of

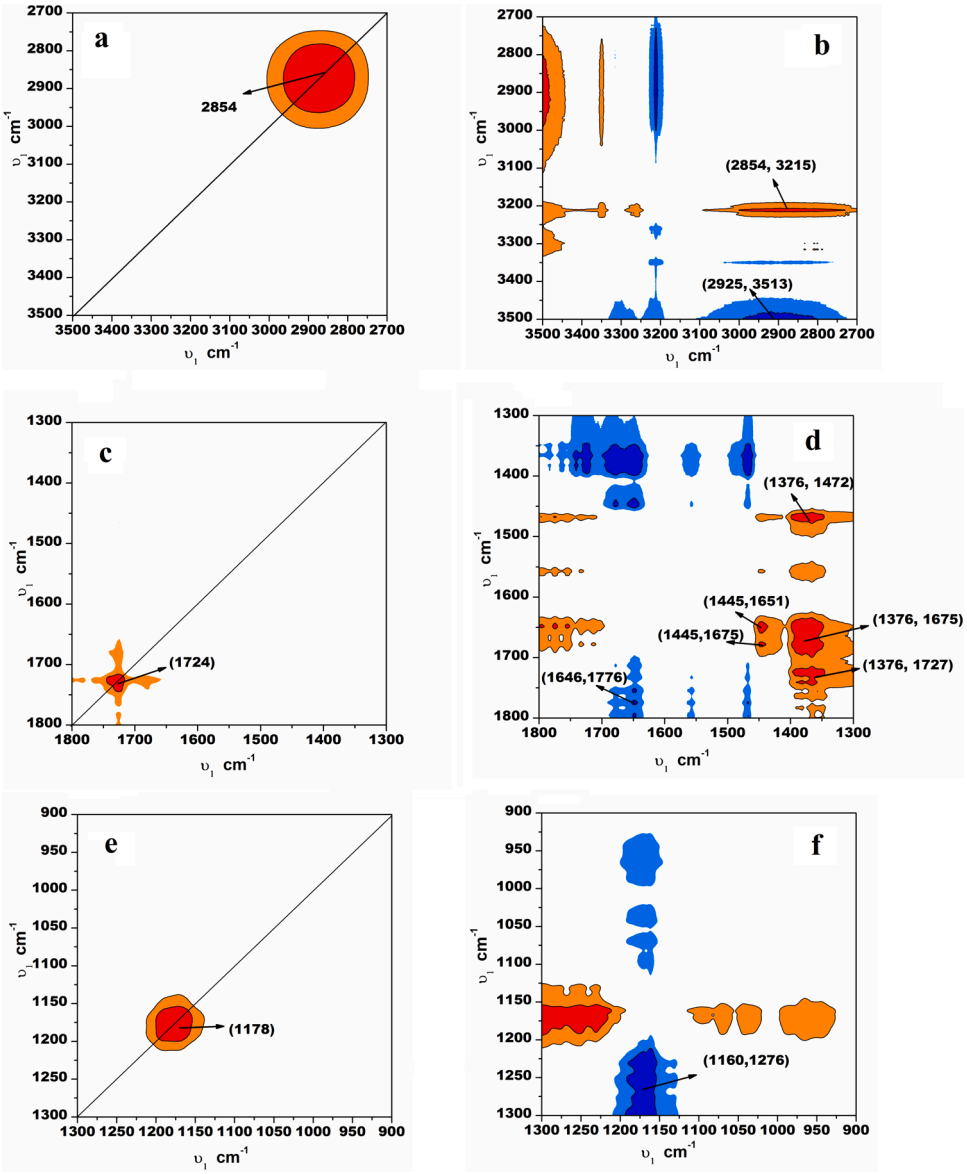

Fig. 3. 2DCOS spectra of *C. convoluta* obtained in the region 3500-2700 cm^{-1}, (a) synchronous (b) asynchronous; in the region 1800-1300 cm^{-1} (c) synchronous (d) asynchronous; in the region 1300-900 cm^{-1} (e) synchronous (f) asynchronous.

Table 2
Pearson's correlation analysis between spectral band areas and physiological parameters.

Pearson correlation coefficient (r)	Lipid peroxidation	Membrane integrity
Carbohydrate band area	0.2894	0.5236*
Protein band area	0.4325	0.5394*
Lipid band area	−0.4234	−0.3403

If the r value is near the ±1; a perfect correlation (increase /if positive) or decrease /if negative).
If the r value is between ±0.50 and ±1; a strong correlation.
If the r value is between ±0.30 and ±0.49; a medium correlation.
If the r value is ±0.29; a small correlation.
When the r value is zero; no correlation.
* Represents a statistically significant difference of $p < 0.05$.

changes in band positions of hydroxyl, carbonyl, and in the amino groups with significant roles in metal chelation. Zhongmin Jin et al. 2020 [1] studied Cd and Pb biosorption of a fungi *S. chinense* QD10 with the spectral biomarkers in the polysaccharide's region using ATR-FTIR spectroscopy. Studies of Fourest et al. [38] and Puranik et al. [39] showed that the divalent metal ion has a high affinity in the microbial biomass. The addition of Pb^{2+} has a stronger impact on the EPS polysaccharides in Trebouxia TR1, decreasing the sugar content, to a lesser extent, as well as altering their monosaccharide composition. The presence of an acidic charge resulted in metal chelation against stress conditions [40,41]. Our results provide evidence of notable differences in the polysaccharides which form the outer barrier responsible for the chelation of metal ions [9]. The various studies reported that free-living algae secrete EPS compositions such as uronic acids that are unique surroundings of the cell [8,16,42]. Leonardo M. Casano [8] studied the impact of Pb on *T* TR1 *and T.* TR9 microalgae which caused changes in proteins and displayed distinct polypeptide patterns. Thus, the conventional FTIR spectra of the band area show variation in the biochemical changes. Due to the complexity in the absorption bands of polysaccharides, it is difficult to identify specific features of functional groups that play a significant role in Pb biosorption. Hence, 2DCOS spectral maps were constructed to give information about specific molecular groups representing the high-level correlation between certain bands. The construction of 2D correlation IR spectra is based on the detection of dynamic changes of a system under an external perturbation (in our study Pb toxicity is taken as external perturbation). The results of 2DCOS provide information about subtle molecular changes occurring in biological samples as detailed in the subsequent section.

3.4. 2D correlation spectral analysis of C. convoluta exposed to Pb treatments

Fig. 3a–f show the synchronous and asynchronous 2DIR spectrum of *C. convoluta* samples in the 3500−2700 cm^{-1}, 1800−1300 cm^{-1}, and 1300−900 cm^{-1} spectral regions. Table 3 shows the respective peaks assigned for synchronous and asynchronous 2DCOS spectra. This region is important because it depicts prominent bands of proteins, lipids, and polysaccharides. Fig. 3a shows a sharp intense auto peak at 2854 cm^{-1} corresponding to CH_2 stretching of the lipids [33]. The asynchronous spectra (Fig. 3b) show both + ve and -ve cross-peaks. The + ve cross peak (2854, 3215) shows changes due to symmetric CH_2 stretching of lipid occurs followed by symmetric OH stretching. The -ve cross peak (2925, 3513) shows changes due to asymmetric CH_2 stretching of lipids that occurs after OH stretching. These correlation changes in spectral frequency are the uniqueness of these 2DCOS spectra which cannot be studied from the conventional FTIR spectra. Further, 2DCOS spectra help us in understanding the biochemical mechanism exhibited by *C. convoluta* due to Pb toxicity.

It is observed from Fig. 3c that the auto peak at 1724 cm^{-1} is

Table 3
Synchronous and asynchronous 2D correlation cross peaks and their assignments for *Cladonia convoluta.*

Synchronous		Asynchronous		
Auto Peaks (cm^{-1})	Assignment	Assignment	Cross Peaks (cm^{-1})	Assignment
2854	Sym CH_2 lipid	Sym CH_2 lipid	+(2854, 3215)	Symmetric OH stretching
		Asym CH_2lipid	-(2925, 3513)	OH stretching
		Pyranose C—H bend/OH bend	+(1376, 1472)	CH_2bending lipids
		Pyranose C—H bend/OH bend	+(1376, 1675)	Amide I proteins β sheet
1724	Polysaccharides/ C-O stretching	Pyranose C—H bend/OH bend	+(1376, 1727)	C = O stretching uronic acid
		δ CH_2 lipids, fatty acids	+(1445, 1651)	Amide I proteins α helix
		δ CH_2 lipids, fatty acids	+(1445, 1675)	Amide I proteins β sheet
		Amide I proteins	-(1646, 1776)	lipids esters
1178	Polysaccharides	Pyranose C—C stretch + CO— stretch + CH deformation	-(1160, 1276)	Amide III proteins

characteristic of polysaccharides due to C—O vibrational stretching [35]. The asynchronous spectra show several + and one -ve cross-peaks (Fig. 3d). The + ve cross-peaks +(1376, 1472), +(1376, 1675), and +(1376, 1727) show the presence of pyranose ring at 1376 cm^{-1} which occurs ahead of the changes in lipids at 1472 cm^{-1}, β sheet of the secondary structure of proteins at 1675 cm^{-1} and uronic acid due to C═O stretching at 1727 cm^{-1} [34]. Thus, significant changes at the pyranose ring occur due to Pb toxicity followed by other biochemical changes. This is because pyranose is simple glucose that occurs due to the synthesis of polysaccharides to meet the immediate requirement of energy in a stress environment. Thus, our study clearly shows changes in pyranose ring observed at 1376 cm^{-1} (Fig. 3d) which cannot be distinguished from conventional FTIR spectra. The other more intense + ve cross-peaks appeared at 1445 cm^{-1} due to CH_2 symmetric bending lipids changes ahead followed by α helix at 1651 cm^{-1} and β sheet at 1675 cm^{-1}, respectively. This indicates a change in secondary structural protein formations (α helix and β sheet), arising from intermolecular hydrogen bond formations in the secondary structure of proteins [43]. The -ve cross-peaks (1646, 1776) show changes in Amide I of proteins after fatty acids of esters in phospholipids. The synchronous and asynchronous spectra in the 1300−900 cm^{-1} region are shown in Fig. 3e and f. The synchronous spectra show an auto peak at 1178 cm^{-1} observed in the 1800−900 cm^{-1} region (Fig. 3e). These auto peaks show the overall susceptibility of polysaccharides when exposed to Pb intoxication as observed from 2DCOS synchronous spectra compared to 1D FTIR spectra. The asynchronous spectra have one negative cross which appeared at 1160 cm^{-1} corresponding to C - C— stretching and CH deformation of pyranose rings which changes after Amide III of proteins at 1276 cm^{-1}. Qiting Xie et al. [44] employed 2DCOS FTIR in studying Cd toxicity in *Chlorella vulgaris* and showed that the carboxylic group of polysaccharides has a higher binding ability compared with other functional groups. It is a key feature for the survival of algae under stress. By using 2DCOS FTIR, Xiaofang Yang et al. [45] showed that the carboxylic C═O group has a high priority of binding to other functional groups.

3.5. 2D hetero correlation spectral analysis of C. convoluta exposed to Pb treatments

Fig. 4a and b show the synchronous and asynchronous hetero correlation maps of *C. convoluta* in the spectral region of 3500−2700 cm^{-1} and 1800−900 cm^{-1}. Synchronous and asynchronous cross-peak assignments of hetero correlation are given in Table 4. The hetero correlation synchronous maps show one + ve cross peaks corresponding to pyranose ring at 1110 cm^{-1} that first occurs and then happens in OH stretching of water molecules at 3406 cm^{-1} (Fig. 4a). This shows that Pb intoxication causes an immediate change in the pyranose ring of simple glucose utilized by lichens to tolerate the Pb toxicity under stress conditions. The hetero asynchronous maps (Fig. 4b) are dominated by several -ve cross-peaks and one + ve cross peak. The -ve cross peak (1572, 3290), (1572, 3130), and (1572,2854) show amide II protein band change at 1572 cm^{-1} happening after amide A and amide B of proteins, and symmetric CH_2 lipids respectively [32,33]. The -ve cross-peaks (1475,3290), (1475,3130), (1475,2854) show changes due to CH_2 lipids at 1475 cm^{-1} occurring after amide A of proteins, amide B of NH stretching, and symmetric stretching of CH_2 lipids. This shows lipids are the next biomolecules affected by the changes occurring in *C. convoluta* due to Pb toxicity. The -ve cross-peaks (1349, 3206) show bands at 1349 cm^{-1} due to pyranose ring changes after OH/NH stretching which occurs at 3206 cm^{-1} [34,35]. The -ve cross-peaks (1206, 3290) show pyranose C—H bending and + OH— bending changes after amide A proteins. The one + cross peak (1051, 3397) shows changes occurring at the glycogen of carbohydrates followed by OH stretching. The various studies show that changes in OH/NH stretching vibrations in algae species are due to the hydroxyl group involved in metal oxygen-binding, indicating a role of the OH group in metal binding [37,46–48].

The results of our study show that polysaccharides, lipids, and proteins play a role in the defense mechanism exhibited by *C. convoluta* under Pb treatment. Further, the order of correlation changes goes from pyranose at 1110 cm^{-1}, followed by CH_2 lipids at 1475 cm^{-1} and then OH/NH stretching at 3206 cm^{-1}. Thus, 2DCOS is a powerful tool showing the correlation changes among the biomolecules due to Pb toxicity. Our results provide information on how lichens respond to Pb toxicity due to possible biosorption. Similar results were obtained by Mecozzi et al. [49] using 2DCOS for marine organic matter related to interactions among carbohydrates, proteins, and lipids. Our study suggests that the cell wall composition of *C. convoluta* interacts with Pb biosorption. This leads to changes occurring in polysaccharides, proteins, and lipids. Veglio & Beolchini [50] identified primary interactive targets for the effect of Cd biosorption on *S. chinense* QD10 as polysaccharides, proteins, and lipids which offer abundant metal-binding functional groups. These dynamic change in the synchronous and asynchronous spectral data shows information concerning features due to perturbation [51].

3.6. Principal Component Analysis (PCA) of C. convoluta exposed to Pb treatments

Fig. 5a shows PCA results obtained for control and various Pb treatments of *Cladonia convoluta*. The plot shows that the samples are separated based on eigenvalues. The first component corresponds to 98 % variation. Component 2 has 2 % variation. The plot shows that the highest eigenvalue was obtained for 2.5 ppb followed by 1 ppb and control. The lowest value was obtained for 0.5 ppb treatment. The difference shows that the samples are separated due to biochemical changes of *C. convoluta* in response to Pb treatment. Fig. 5b shows PCA loadings plotted against wavenumber. The highest positive loadings values at 1035 cm^{-1} correspond to the C—C stretching of the pyranose ring. The -ve loading value at 914 cm^{-1} shows changes in glucan band (α anomer CH deformation) of polysaccharides. This shows polysaccharide synthesis by *C. convoluta* to meet immediate energy needs under stress conditions.

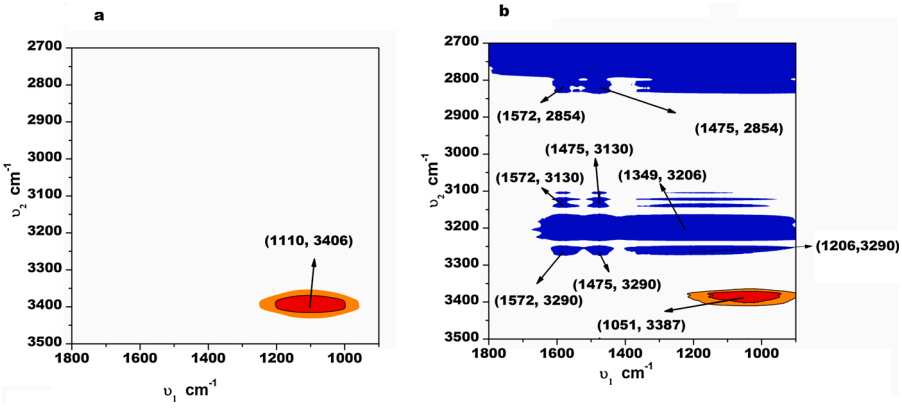

Fig. 4. 2DCOS hetero correlation spectra of *C. convoluta* (a) Synchronous (b) Asynchronous.

Table 4
Synchronous and asynchronous 2D hetero correlation cross peaks and their assignments for *Cladonia convoluta.*

Synchronous			Asynchronous		
Assignment	Cross Peaks (cm^{-1})	Assignment	Assignment	Cross Peaks (cm^{-1})	Assignment
Pyranose ring C-C stretch + C-O stretch + CH deformation	+(1110, 3406)	OH stretching	Amide II proteins	-(1572,3290)	Amide A proteins
			Amide II proteins	-(1572,3130)	Amide B NH stretching
			Amide II proteins	-(1572,2854)	Sym CH_2 lipid
			Proteins, lipids (CH_2)	-(1475, 3290)	Amide A proteins
			Proteins, lipids (CH_2)	-(1475,3130)	Amide B NH stretching
			Proteins, lipids (CH_2)	-(1475,2854)	Sym CH_2 lipid
			Pyranose ring C—C stretch	-(1206,3290)	Amide A proteins
			Pyranose C—H bending + OH— bending)	-(1349, 3206)	OH stretching
			Glycogen	+(1051, 3397)	OH stretching

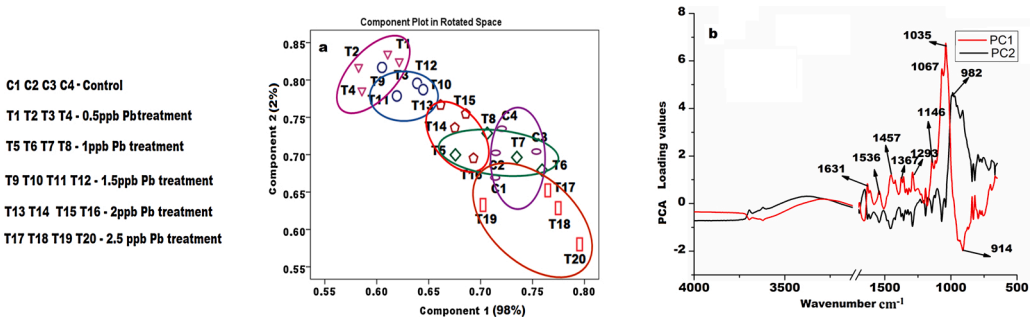

Fig. 5. (a) PCA scatter plots of *C. convoluta* of control and various Pb treatments. (b) Variation of the factor loading obtained from the PCA with the corresponding wavenumber.

3.7. Hierarchical cluster analysis (HCA) of C. convoluta exposed to Pb treatments

The HCA dendrogram of *C. convoluta* exposed to various Pb treatments is shown in Fig. 6a. Cluster 1 arises with a grouping of two subclusters 5 and 6 which are closer to each other. The clusters 5 and 6 correspond to the control and treated samples separated by a smaller range of 4–10. Cluster 2 results from a grouping of two well-differentiated subclusters 3 and 4. It is separated by distance in the range of 4–8, significantly. The results show samples are well separated between two major clusters (Cluster 1 and Cluster 2). They have high values in the range of 10–25 which is reflected in the dendrogram scale. Thus, the dendrogram depicts clustering of samples, with the identical samples having a shorter distance between them. Similar effective differentiation was obtained by R. da Silva Leite et al. [24], Gupta et al. [25,52], and Cao Z et al. [53] for plants, microorganisms, and medicinal plants, respectively through HCA from FTIR spectra.

3.8. Receiver operation characteristics (ROC) analysis of C. convoluta exposed to Pb treatments

Fig. 6b shows the ROC curve for various Pb treatments. The diagnostic ability was measured by the area under the curve (AUC). As a general rule, the measured AUC in the upper left-hand side provides good reliability of the test. Our results lie in the range of 0.944−0.966. The highest ROC curve area was obtained for 0.5 ppb of Pb and the lowest value for 2.0 ppb of Pb treatments. The results from AUC show the good reliability of our study. R. da Silva Leite et al. [24], and Gupta et al. [25,52] employed ROC analysis of infrared spectroscopy to validate the accuracy of experiments in biological populations. The study confirms the overall reliability of the test carried out from the available experimental data.

4. Conclusion

Our results indicate a prominent spectral change observed in polysaccharides which is the major component in *C. convoluta*. It shows bioabsorption of Pb on lichens and throws new insights into the defense mechanisms as studied by 2DCOS FTIR. The auto peak from synchronous spectra shows prominent changes observed at lipids and polysaccharides. Further presence of + ve cross-peaks at 1675 cm^{-1} shows β sheet secondary structure of protein due to Pb exposure. The dynamic change in spectral data in the asynchronous maps shows the correlation changes occurring between pyranose rings at 1376 cm^{-1} followed by lipids (1472 cm^{-1}) and proteins (1675 cm^{-1}). This helps in understanding the tolerance mechanism exhibited by the species under the external environment. Thus, it provides a pathway of understanding the effective bioremediation process occurring in them. PCA results for control and various Pb treatments show samples are well separated based on biochemical changes. The high value of area under the curve from ROC analysis supports our findings showing good reliability of the study. Further 2DCOS correlation spectra remarkably enhanced the resolution of IR spectra in obtaining information regarding intermolecular and intramolecular interactions between functional groups and relative intensity changes due to Pb intoxication. In this way, 2DCOS IR is a vital tool in depicting characteristic changes in biochemical compositions occurring in lichens species due to Pb intoxication.

CRediT authorship contribution statement

Rafig Gurbanov: Conceptualization. **Sivakumaran Karthikeyan**, **Rafig Gurbanov:** Data curation; Formal analysis. **Sivakumaran Karthikeyan**, **Dilek Unal**, **Rafig Gurbanov:** Investigation. **Rafig Gurbanov**, **Dilek Unal:** Experiment Methodology. **Rafig Gurbanov**, **Dilek Unal:** Resources. **Sivakumaran Karthikeyan**, **Rafig Gurbanov:** Software. **Rafig Gurbanov**: Supervision. **Sivakumaran Karthikeyan**, **Rafig**

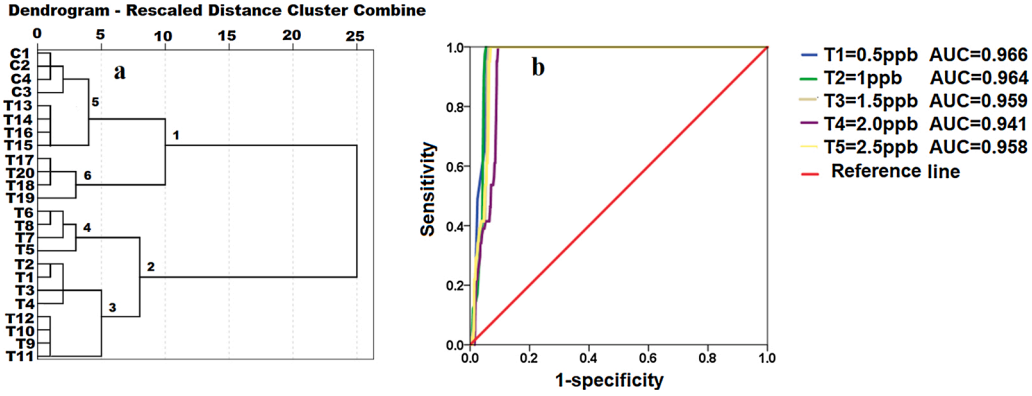

Fig. 6. (a) Dendrogram of *C. convoluta* of control and various Pb treatments showing group linkage obtained using ward algorithm (b) Receiver operating characteristics curve of various Pb treatments for *C. convoluta*.

Gurbanov: Validation. **Sivakumaran Karthikeyan**, **Rafig Gurbanov:** Writing - original draft. **Sivakumaran Karthikeyan**, **Dilek Unal**, **Rafig Gurbanov:** Writing - review & editing.

Declaration of Competing Interest

The authors have declared no conflict of interest.

References

[1] Z. Jin, L. Xie, T. Zhang, L. Liu, T. Black, K.C. Jones, H. Zhang, X. Wang, N. Jin, D. Zhang, Interrogating cadmium and lead biosorption mechanisms by Simplicillium chinense via infrared spectroscopy, Environ. Pollut. 263 (2020) 114419, https://doi.org/10.1016/j.envpol.2020.114419.

[2] X. Lin, Y.-J. Cai, Z.-X. Li, Q. Chen, Z.-L. Liu, R. Wang, Structure determination, apoptosis induction, and telomerase inhibition of CFP-2, a novel lichenin from Cladonia furcata, Biochim. Biophys. Acta 1622 (2003) 99–108, https://doi.org/10.1016/s0304-4165(03)00131-4.

[3] S.E. Bailey, T.J. Olin, R.M. Bricka, D.D. Adrian, A review of potentially low-cost sorbents for heavy metals, Water Res. 33 (1999) 2469–2479, https://doi.org/10.1016/S0043-1354(98)00475-8.

[4] G. Shrestha, L.L. St Clair, K.L. O'Neill, The immunostimulating role of lichen polysaccharides: a review, Phytother. Res. 29 (2015) 317–322, https://doi.org/10.1002/ptr.5251.

[5] B. Li, Y. Cai, C. Qi, R. Hansen, C. Ding, T.C. Mitchell, J. Yan, Orally administered particulate beta-glucan modulates tumor-capturing dendritic cells and improves antitumor T-cell responses in cancer, Clin. Cancer Res. Off. J. Am. Assoc. Cancer Res. 16 (2010) 5153–5164, https://doi.org/10.1158/1078-0432.CCR-10-0820.

[6] J. Baran, D.J. Allendorf, F. Hong, G.D. Ross, Oral beta-glucan adjuvant therapy converts nonprotective Th2 response to protective Th1 cell-mediated immune response in mammary tumor-bearing mice, Folia Histochem. Cytobiol. 45 (2007) 107–114.

[7] M. Eder, U. Lütz-Meindl, Pectin-like carbohydrates in the green alga Micrasterias characterized by cytochemical analysis and energy filtering TEM, J. Microsc. 231 (2008) 201–214, https://doi.org/10.1111/j.1365-2818.2008.02036.x.

[8] L.M. Casano, M.R. Braga, R. Álvarez, E.M. del Campo, E. Barreno, Differences in the cell walls and extracellular polymers of the two Trebouxia microalgae coexisting in the lichen Ramalina farinacea are consistent with their distinct capacity to immobilize extracellular Pb, Plant Sci. 236 (2015) 195–204, https://doi.org/10.1016/j.plantsci.2015.04.003.

[9] S. Ozturk, B. Aslim, Z. Suludere, S. Tan, Metal removal of cyanobacterial exopolysaccharides by uronic acid content and monosaccharide composition, Carbohydr. Polym. 101 (2014) 265–271, https://doi.org/10.1016/j.carbpol.2013.09.040.

[10] Z.M. Şenol, Ü.D. Gül, R. Gurbanov, S. Şimşek, Optimization the removal of lead ions by fungi: explanation of the mycosorption mechanism, J. Environ. Chem. Eng. 9 (2021) 104760, https://doi.org/10.1016/j.jece.2020.104760.

[11] A. Deveau, A. Kohler, P. Frey-Klett, F. Martin, The major pathways of carbohydrate metabolism in the ectomycorrhizal basidiomycete Laccaria bicolor S238N, New Phytol. 180 (2008) 379–390, https://doi.org/10.1111/j.1469-8137.2008.02581.x.

[12] D.J. Adams, Fungal cell wall chitinases and glucanases, Microbiology 150 (2004) 2029–2035, https://doi.org/10.1099/mic.0.26980-0.

[13] C. Arthur, Linkage Analysis and Compositional Studies of β- Glucan From Saccharomyces cerevisiae and Compositional Studies of Mannan from Candida Albicans, East Tennessee State University, 2015. https://dc.etsu.edu/etd/2537.

[14] R. Gurbanov, N.S. Ozek, S. Tunçer, F. Severcan, A.G. Gozen, Aspects of silver tolerance in bacteria: infrared spectral changes and epigenetic clues, J. Biophotonics 11 (2018), https://doi.org/10.1002/jbio.201700252.

[15] R. Gurbanov, S. Tunçer, S. Mingu, F. Severcan, A.G. Gozen, Methylation, sugar puckering and Z-form status of DNA from a heavy metal-acclimated freshwater Gordonia sp, J. Photochem. Photobiol. B, Biol. 198 (2019) 111580, https://doi.org/10.1016/j.jphotobiol.2019.111580.

[16] R. Gurbanov, D. Unal, The biomolecular alterations in cladonia convoluta in response to lead exposure, Spectrosc. Lett. 51 (2018) 563–570, https://doi.org/10.1080/00387010.2018.1533564.

[17] R.L. Heath, L. Packer, Photoperoxidation in isolated chloroplasts. I. Kinetics and stoichiometry of fatty acid peroxidation, Arch. Biochem. Biophys. 125 (1968) 189–198, https://doi.org/10.1016/0003-9861(68)90654-1.

[18] J. Garty, O. Tamir, Y. Cohen, H. Lehr, A.I. Goren, Changes in the potential quantum yield of photosystem II and the integrity of cell membranes relative to the elemental content of the epilithic desert lichen Ramalina maciformis, Environ. Toxicol. Chem. 21 (2002) 848–858, https://doi.org/10.1897/1551-5028(2002)021<0848:citpqy>2.0.co;2.

[19] I. Noda, Generalized two-dimensional correlation method applicable to infrared, Raman, and other types of spectroscopy, Appl. Spectrosc. 47 (1993) 1329–1336. http://as.osa.org/abstract.cfm?URI=as-47-9-1329.

[20] I. Noda, A.E. Dowrey, C. Marcoli, G.M. Story, Y. Ozaki, Generalized two-dimensional correlation spectroscopy, Appl. Spectrosc. 54 (2000) 236A–248A. http://as.osa.org/abstract.cfm?URI=as-54-7-236A.

[21] I. Noda, Y. Ozaki, Two-dimensional Correlation Spectroscopy-Applications in Vibrational and Optical Spectroscopy, John Wiley & Sons, Chichester, England, 2004, https://doi.org/10.1002/0470012404.

[22] I. Noda, Modified two-dimensional correlation spectra for streamlined determination of sequential order of intensity variations, J. Mol. Struct. 1124 (2016) 197–206, https://doi.org/10.1016/j.molstruc.2016.01.092.

[23] Y. Park, S. Jin, I. Noda, Y.M. Jung, Emerging developments in two-dimensional correlation spectroscopy (2D-COS), J. Mol. Struct. 1217 (2020) 128405, https://doi.org/10.1016/j.molstruc.2020.128405.

[24] R. da Silva Leite, K. Sivakumaran, S. Hernandéz-Navarro, M. Neves do Nascimento, N.M.R. Potosme, P. Carrión-Prieto, E.D.S. Souza, Nitrogen influenced biomolecular changes on Physalis L. species studied using 2DCOS spectral analysis coupled with chemometric and Receiver operation characteristics analysis, Spectrochim. Acta A. Mol. Biomol. Spectrosc. 249 (2021) 119220, https://doi.org/10.1016/j.saa.2020.119220.

[25] A.D. Gupta, E. Kavitha, S. Singh, S. Karthikeyan, Toxicity mechanism of Cu(2+) ion individually and in combination with Zn(2+) ion in characterizing the molecular changes of Staphylococcus aureus studied using FTIR coupled with chemometric analysis, J. Biol. Phys. 46 (2020) 395–414, https://doi.org/10.1007/s10867-020-09560-7.

[26] J.H.J. Ward, Hierarchical grouping to optimize an objective function, J. Am. Stat. Assoc. 58 (1963) 236–244, https://doi.org/10.1080/01621459.1963.10500845.

[27] N. Karakoti, R. Bajpai, D.K. Upreti, G.K. Mishra, A. Srivastava, S. Nayaka, Effect of metal content on chlorophyll fluorescence and chlorophyll degradation in lichen Pyxine cocoes (Sw.) Nyl.: a case study from Uttar Pradesh, India, Environ. Earth Sci. 71 (2014) 2177–2183, https://doi.org/10.1007/s12665-013-2623-5.

[28] M.H. Wierzbicka, E. Przedpełska, R. Ruzik, L. Ouerdane, K. Połeć-Pawlak, M. Jarosz, J. Szpunar, A. Szakiel, Comparison of the toxicity and distribution of cadmium and lead in plant cells, Protoplasma 231 (2007) 99–111, https://doi.org/10.1007/s00709-006-0227-6.

[29] Z.Z. Yan, L. Ke, N.F.Y. Tam, Lead stress in seedlings of Avicennia marina, a common mangrove species in South China, with and without cotyledons, Aquat. Bot. 92 (2010) 112–118, https://doi.org/10.1016/j.aquabot.2009.10.014.

[30] R. Álvarez, A. del Hoyo, C. Díaz-Rodríguez, A.J. Coello, E.M. del Campo, E. Barreno, M. Catalá, L.M. Casano, Lichen rehydration in heavy metal-polluted environments: Pb modulates the oxidative response of both Ramalina farinacea thalli and its isolated microalgae, Microb. Ecol. 69 (2015) 698–709, https://doi.org/10.1007/s00248-014-0524-0.

[31] A. Dzubaj, M. Bačkor, J. Tomko, E. Peli, Z. Tuba, Tolerance of the lichen Xanthoria parietina (L.) Th. Fr. to metal stress, Ecotoxicol. Environ. Saf. 70 (2008) 319–326, https://doi.org/10.1016/j.ecoenv.2007.04.002.

[32] A.F. Meisurova, S.D. Khizhnyak, P.M. Pakhomov, IR spectral analysis of the chemical composition of the lichen Hypogymnia physodes to assess atmospheric pollution, J. Appl. Spectrosc. 76 (2009) 420–426, https://doi.org/10.1007/s10812-009-9179-x.

[33] B.R. Shakya, P. Shrestha, H.-R. Teppo, L. Rieppo, The use of Fourier Transform Infrared (FTIR) spectroscopy in skin cancer research: a systematic review, Appl. Spectrosc. Rev. 56 (2021) 347–379, https://doi.org/10.1080/05704928.2020.1791152.

[34] K. Naseer, S. Ali, J. Qazi, ATR-FTIR spectroscopy as the future of diagnostics: a systematic review of the approach using bio-fluids, Appl. Spectrosc. Rev. 56 (2021) 85–97, https://doi.org/10.1080/05704928.2020.1738453.

[35] V. Mohaček-Grošev, R. Božac, G.J. Puppels, Vibrational spectroscopic characterization of wild growing mushrooms and toadstools, Spectrochim. Acta Part A Mol. Biomol. Spectrosc. 57 (2001) 2815–2829, https://doi.org/10.1016/S1386-1425(01)00584-4.

[36] E. Skotti, S. Kountouri, P. Bouchagier, D.I. Tsitsigiannis, M. Polissiou, P. A. Tarantilis, FTIR spectroscopic evaluation of changes in the cellular biochemical composition of the phytopathogenic fungus Alternaria alternata induced by extracts of some Greek medicinal and aromatic plants, Spectrochim. Acta A. Mol. Biomol. Spectrosc. 127 (2014) 463–472, https://doi.org/10.1016/j.saa.2014.02.113.

[37] L. D'Souza, P. Devi, D.M.P. Shridhar, C.G. Naik, Use of Fourier Transform Infrared (FTIR) spectroscopy to study cadmium-induced changes in Padina tetrastromatica (Hauck), Anal. Chem. Insights 3 (2008) 135–143.

[38] E. Fourest, C. Canal, J.C. Roux, Improvement of heavy metal biosorption by mycelial dead biomasses (Rhizopus arrhizus, Mucor miehei and Penicillium chrysogenum): pH control and cationic activation, FEMS Microbiol. Rev. 14 (1994) 325–332, https://doi.org/10.1111/j.1574-6976.1994.tb00106.x.

[39] P.R. Puranik, J.M. Modak, K.M. Paknikar, A comparative study of the mass transfer kinetics of metal biosorption by microbial biomass, Hydrometallurgy 52 (1999) 189–197, https://doi.org/10.1016/S0304-386X(99)00017-1.

[40] S. Pereira, A. Zille, E. Micheletti, P. Moradas-Ferreira, R. De Philippis, P. Tamagnini, Complexity of cyanobacterial exopolysaccharides: composition, structures, inducing factors and putative genes involved in their biosynthesis and assembly, FEMS Microbiol. Rev. 33 (2009) 917–941, https://doi.org/10.1111/j.1574-6976.2009.00183.x.

[41] A. Mishra, K. Kavita, B. Jha, Characterization of extracellular polymeric substances produced by micro-algae Dunaliella salina, Carbohydr. Polym. 83 (2011) 852–857, https://doi.org/10.1016/j.carbpol.2010.08.067.

[42] G.-P. Sheng, H.-Q. Yu, X.-Y. Li, Extracellular polymeric substances (EPS) of microbial aggregates in biological wastewater treatment systems: a review, Biotechnol. Adv. 28 (2010) 882–894, https://doi.org/10.1016/j.biotechadv.2010.08.001.

[43] M. Mecozzi, E. Sturchio, Effects of essential oil treatments on the secondary protein structure of Vicia faba: a mid-infrared spectroscopic study supported by two-dimensional correlation analysis, Spectrochim. Acta A. Mol. Biomol. Spectrosc. 137 (2015) 90–98, https://doi.org/10.1016/j.saa.2014.08.020.

[44] Q. Xie, N. Liu, D. Lin, R. Qu, Q. Zhou, F. Ge, The complexation with proteins in extracellular polymeric substances alleviates the toxicity of Cd (II) to Chlorella vulgaris, Environ. Pollut. 263 (2020) 114102, https://doi.org/10.1016/j.envpol.2020.114102.

[45] X. Yang, X. Zheng, L. Wu, X. Cao, Y. Li, J. Niu, F. Meng, Interactions between algal (AOM) and natural organic matter (NOM): impacts on their photodegradation in surface waters, Environ. Pollut. 242 (2018) 1185–1197, https://doi.org/10.1016/j.envpol.2018.07.099.

[46] J. Guo, X. Zhang, Metal-ion interactions with sugars. The crystal structure and FTIR study of an SrCl2-fructose complex, Carbohydr. Res. 339 (2004) 1421–1426, https://doi.org/10.1016/j.carres.2004.03.004.

[47] P. Blokker, S. Schouten, H. van den Ende, J.W. de Leeuw, P.G. Hatcher, J. S. Sinninghe Damsté, Chemical structure of algaenans from the fresh water algae Tetraedron minimum, Scenedesmus communis and Pediastrum boryanum, Org. Geochem. 29 (1998) 1453–1468, https://doi.org/10.1016/S0146-6380(98)00111-9.

[48] D.C. Sigee, A. Dean, E. Levado, M.J. Tobin, Fourier-transform infrared spectroscopy of Pediastrum duplex: characterization of a micro-population isolated from a eutrophic lake, Eur. J. Phycol. 37 (2002) 19–26, https://doi.org/10.1017/S0967026201003444.

[49] M. Mecozzi, E. Pietrantonio, M. Pietroletti, The roles of carbohydrates, proteins and lipids in the process of aggregation of natural marine organic matter investigated by means of 2D correlation spectroscopy applied to infrared spectra, Spectrochim. Acta Part A Mol. Biomol. Spectrosc. 71 (2009) 1877–1884, https://doi.org/10.1016/j.saa.2008.07.015.

[50] F. Veglio', F. Beolchini, Removal of metals by biosorption: a review, Hydrometallurgy 44 (1997) 301–316, https://doi.org/10.1016/S0304-386X(96)00059-X.

[51] M. Mecozzi, M. Pietroletti, R. Di Mento, Application of FTIR spectroscopy in ecotoxicological studies supported by multivariate analysis and 2D correlation spectroscopy, Vib. Spectrosc. 44 (2007) 228–235, https://doi.org/10.1016/j.vibspec.2006.11.006.

[52] A.D. Gupta, S. Karthikeyan, A. Chitra, Resistance mechanism of Ni 2+ ion individually and in combination with the Cr 6+ ion in Staphylococcus aureus species to characterize the molecular changes studied using infrared spectroscopy coupled with chemometrics, Infrared Phys. Technol. 94 (2018) 126–133, https://doi.org/10.1016/j.infrared.2018.09.002.

[53] Z. Cao, Z. Wang, Z. Shang, J. Zhao, Classification and identification of Rhodobryum roseum Limpr. and its adulterants based on fourier-transform infrared spectroscopy (FTIR) and chemometrics, PLoS One 12 (2017) e0172359, https://doi.org/10.1371/journal.pone.0172359.